International Journal of Mechanical and Production Engineering Research and Development (IJMPERD)
ISSN (P): 2249–6890; ISSN (E): 2249–8001
Vol. 10, Issue 2, Apr 2020, 737–746

EXCITATION MODEL AND MOTION ANALYSIS OF THE VIBRATORY BOWL FEEDER

KANG-YUL BAE[1] & BONG-HWAN KIM[2]

[1]*Department of Mechatronics Engineering, Gyeongnam National University of Science and Technology, Jinju, Korea*

[2]*Department of Automotive Engineering, Gyeongnam National University of Science and Technology, Jinju, Korea*

ABSTRACT

In the design of a vibratory bowl feeder to produce the desired part feed rate, motion analyses are necessary on both the bowl and the part during excitation of the bowl feeder. This study modelled the excitation force of the electromagnet that gives a vibratory motion to the bowl feeder. The model showed that the excitation force increased linearly with the amplitude of the excitation voltage, whereas the force decreased parabolically with the increment of frequency. The force model was then applied to the equation of motion for the motion analysis of the bowl. The motion of the part was finally modelled to be associated with the result of the bowl motion. The model of part motion was analyzed to reveal that the feed rate increased with the reduction of frequency, and also increased with enlarging the magnitude of the excitation voltage. It was also illustrated that in the high feed rate, the part travelled mainly with jump motion, while in the low feed rate, it travelled with slip motion. The model proposed in this study can be used in the optimal design of various bowl feeders.

KEY WORDS: Bowl Feeder, Excitation Model, Motion Analysis, Feed Rate & Excitation Parameters

Received: Oct 22, 2019; **Accepted**: Nov 12, 2019; **Published**: Mar 25, 2020; **Paper Id.**: IJMPERDAPR202073

Original Article

1. INTRODUCTION

The vibratory bowl feeder has been widely utilized as one of the part feeder units to load, feed, and align parts in an exact and precise way for the automation of assembly production in the automotive and home appliance industries, etc. (Deshmukh, 2017). Figure 1(a) shows the bowl feeder, which typically consists of a bowl, a base, leaf springs, and rubber feet (Boothroyd et al, 1982). The bowl has a hopper to load parts at the center, an inclined track at the outskirt to feed parts, and is supported by 4 inclined leaf springs attached to the base. Figure 1(b) shows that an electromagnet is located in between the bowl and base, which would be excited by an alternating current power source. Because the electromagnet attached on the base produces an attractive force to pull the bowl toward the base and diminishes the force periodically in a condition that the leaf springs positioned between the bowl and base constrain the bowl movement, the bowl simultaneously vibrates in the vertical and horizontal directions.

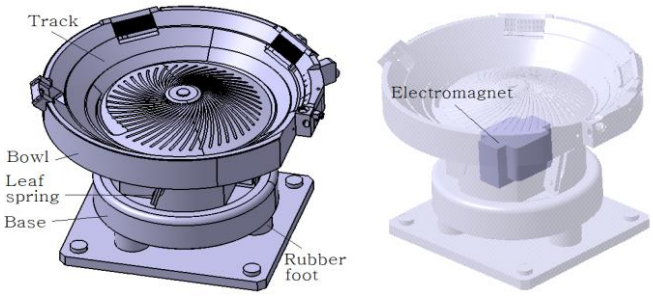

(a) Bowl feeder (b) Electromagnet

Figure 1: Schematic Drawing of the Bowl Feeder.

To decide the feed rate of parts in the design of a vibratory bowl feeder, analyses in advance of the motion of the bowl and parts are necessary. The motion of parts had been mainly analyzed with respect to a predefined bowl motion, such as harmonic oscillation (Boothroyd et al, 1982; Han et al, 1996; Kim et al, 1996). In particular, Han et al. suggested a nonlinear dynamic model to consider the repeated collision of parts moving on the track, and reported the results of the numerical analysis on the part feed rate (Han et al, 1996). Hsieh et al. proposed a new excitation method for the bowl with a motor and Old-ham coupling mechanism, and performed a kinematic analysis to show the method was effective to move parts (Hsieh et al, 2013). Ashrafizadeh et al. considered the part on a bowl feeder not as a particle, but as a hexahedron to have 3 degrees of freedom, and then analyzed the travel motion numerically with variation of the operation parameters (Ashrafizadeh et al, 2013). Deshmukh studied the variation of the part feed rate with the change of applied voltage, number of parts, and length of part (Deshmukh, 2017). Meanwhile, Maul suggested a dynamic model of the bowl itself using mass-spring-damper elements, and also derived the motion equation to predict the movement of a part on the bowl to predict the part feed rate (Maul et al, 1997). However, the excitation model to vibrate the bowl was not presented; also, there were no results with respect to the change of excitation of the electromagnet. Kim et al. sought to reveal experimentally the relation between the applied voltage and air gap of the electromagnet and the part feed rate (Kim et al, 1996). Sturm et al. carried out a dynamic analysis with a mass-spring-damper model for a bowl feeder that utilized 3 electromagnets to provide the excitation (Sturm et al, 2017).

In this study, a small vibratory bowl feeder as shown in figure 1 was proposed to feed a thin disc with a thickness of 50 μm. In the design to implement the proposed feeder, the relation between the excitation of an electromagnet, the behavior of a bowl feeder, and the analysis of a part movement were needed. For this purpose, the excitation model of an electromagnet was developed and the model was then integrated into the dynamic model of a bowl feeder suggested by Maul et al. Taking into account the relation between the excitation force and operation parameters, the motion analyses of the bowl and the part were then carried out with change of the parameters, to evaluate the performance of the bowl feeder.

2. EXCITATION FORCE AND DYNAMICS MODELS OF THE BOWL FEEDER

2.1. Excitation Force Model

Figure 2 shows the configuration of the electromagnet to excite the bowl for feeding the part on its track in a vibratory bowl feeder. The magnet consists of a lower core wound with the excitation coil, and an upper core, which are attached to the bowl and base, respectively.

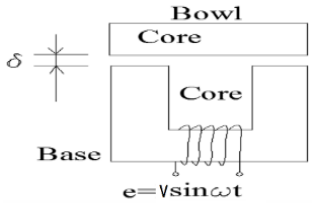

Figure 2: Configuration of the Electromagnet of the Vibratory Bowl Feeder.

With the electric energy supplied to the coil, the electromagnetic energy (W_m) accumulated in the magnetic field can be expressed as follows:

$$W_m = \int_0^i Lidi = \frac{1}{2}Li^2 = \frac{1}{2}(Ni)^2 R_m^{-1} \quad (1)$$

where, the magnetic resistance R_m is defined as follows:

$$R_m = \frac{l_i}{\mu_i S}\left(1 + \mu_s \frac{l_g}{l_i}\right) = m(1 + n\delta)\ ;\ \mathrm{m} \equiv \frac{l_i}{\mu_i S}\ ;\ \mathrm{n} \equiv \frac{2\mu_s}{l_i} \quad (2)$$

where, L is the inductance, i is the current, N is the number of coil turns, l_i and $l_g(=2\delta)$ are the length of the core and air gap, respectively, μ_i and μ_s are the permeability of air and relative permeability of the core, respectively, and S is the sectional area of the core. The attractive force, i.e., the excitation force (F_d) inducing the vibration of the bowl, can be derived by the derivative of the electromagnet energy with respect to the displacement, as follows (Lee et al, 1979):

$$F_d = \frac{dW_m}{d\delta} = -\frac{1}{2}(Ni)^2 \frac{n}{m(1+n\delta)^2} \quad (3)$$

Meanwhile, the current i can be presented as follows:

$$i = Isin(\omega t - \theta)\ ;\ i^2 = \frac{1}{2}I^2\left(1 - cos2(\omega t - \theta)\right) \quad (4)$$

where, ω is the angular frequency of the excitation voltage. The electromagnet system can be assumed to be an equivalent circuit consisting of the electric resistance (R) and the inductance (L) in series. The analysis of this circuit produces an equation to calculate the magnitude of the current flowing through the magnet (Park, 1994). The magnitude is calculated from $I = V/Z$, where, V is the magnitude of enforced voltage, $Z = \sqrt{R^2 + X_L^2}$ is the impedance of the magnet system, and $X_L = \omega L$. The phase difference is expressed as follows: $\theta = tan^{-1}(\frac{X_L}{R})$. Therefore, the excitation force can finally be modelled as follows:

$$F_d = -\frac{1}{4}(NI)^2 \frac{n}{m(1+n\delta)^2}(1 - cos2(\omega t - \theta)) \quad (5)$$

2.2. Dynamics Model of Bowl and Part

To analyze the dynamics of the bowl feeder, the base coordinate system $(\theta_1 - y_1)$ and the bowl coordinate system $(\theta_2 - y_2)$ were defined as shown in Fig. 3(a). In the figure, the vertical and angular displacements of the base are presented as y_1 and θ_1, respectively, the vertical and angular displacements of the bowl as y_2 and θ_2, respectively, and the deflection of the leaf spring as d. The mass of the base is m_1, the mass of the bowl is m_2, and the radial connection positions between the leaf spring and base and between the leaf spring and bowl are r_1 and r_2, respectively. The inclined angle of leaf spring to the horizontal plane is presented as α. With the geometric relations and definitions, the vertical and angular displacements of the bowl can be related to those of the base as follows:

$$y_2 = y_1 + dcos\alpha \; ; \; \theta_2 = \theta_1 + \frac{d}{r_2} sin\alpha \quad (6)$$

Figure 3(b) shows the force acting on each element of the bowl feeder, where, F_d is the attractive force, F_a and F_b are the axial and deflection forces on the leaf spring, respectively, and F_v and F_h are the vertical and horizontal reaction forces on each rubber foot, respectively.

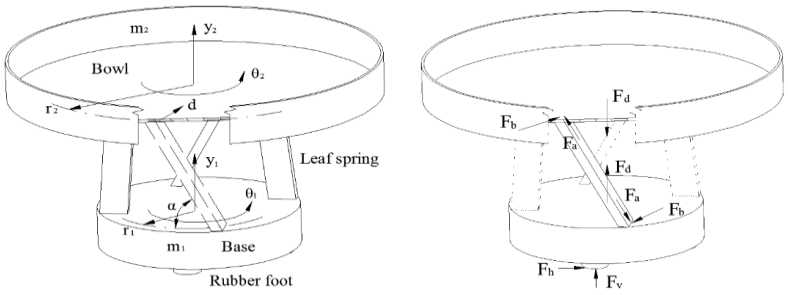

(a) Coordinate Systems for Bowl and Base (b) Force on Element

Figure 3: Configuration of the Bowl Feeder.

Figure 4 shows that in order to relate the part motion to the bowl motion, a local coordinate $u - v$ was introduced in the inclined track of the bowl, where the u and v directions are parallel and vertical to the track surface, respectively, which is inclined to the horizon at an angle of $\emptyset$.

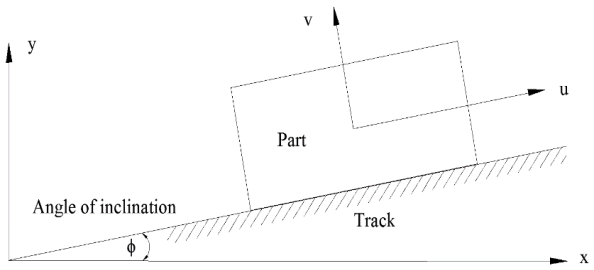

Figure 4: Relation Between the Global and Local Coordinate Systems on the Track.

Therefore, using the relation $[T]$ between the bowl and base positions, a track position in the $u-v$ coordinate system can be expressed with the base coordinate (y_1, θ_1) and the leaf spring displacement (d):

$$\begin{bmatrix} u \\ v \end{bmatrix} = [T] \begin{bmatrix} y_1 \\ \theta_1 \\ d \end{bmatrix} \tag{7}$$

Finally, the equation for base motion can be derived in the form of a state equation as shown in Fig. 5(a) (Maul et al, 1997). In the equation, $\mathbf{M}$ is the inertia matrix, $\mathbf{K}$ is the stiffness matrix, $\mathbf{B}$ is the damping matrix, and $\mathbf{U}$ is the direction vector. The solution of the equation can be presented as follows:

$$X = \begin{bmatrix} Y \\ \dot{Y} \end{bmatrix}, \ \mathrm{Y} = \begin{bmatrix} y_1 \\ \theta_1 \\ d \end{bmatrix} \tag{8}$$

The components of the vector $\mathbf{Y}$ are vertical (y_1) and rotational (θ_1) displacements of the base, and deflection (d) of the leaf spring, respectively. The vector X has the components of Y and derivative of Y. Therefore, when the differential equation is solved, the displacement and velocity of bowl can be calculated with Eq. (6), and the acceleration of bowl is then obtained with the change from the velocity of the previous step. When the motion of the bowl is presented in the track coordinates, using the motion equation for the part developed with the free body diagram, the motion of the part moving on the track can be described.

Just before slipping, the part contacts with the track to be in a static friction state, and moves along with the track. When the part begins to move relatively by slipping on the track, the part gets to be in the state of dynamic friction with the track. When the track has a big acceleration in the negative direction of the v axis, the part then has a motion to fall freely. Each load condition on the part moving on the track can be illustrated as shown in Fig. 6, where, m_p is the part mass, $\mathbf{N}$ is the contact force, $\mathbf{F}$ is the friction force, and $\mathbf{g}$ is gravity. Figure 6(a) shows a state in which the part moves forward relatively slipping on the track, or a state just before the part starts to move forward (μ_s and μ_k are the static and dynamic friction coefficients, respectively). Figure 6(b) shows a state in which the part moves backward, or a state just before the

part starts to move backward. Figure 6(c) shows a state in which the part moves on the track by jumping. That is, the motion equations for the part are derived differentially according to the motion of the bowl, and they are expressed and utilized case-by-case, as shown in Fig. 5(b). When the acceleration of the part is determined, accumulation of the acceleration during the time interval produces the increment of velocity. The increment is then added to the previous velocity of step t to give the velocity $(\dot{u}_p, \dot{v}_p)$ of the current step $(t+1)$.

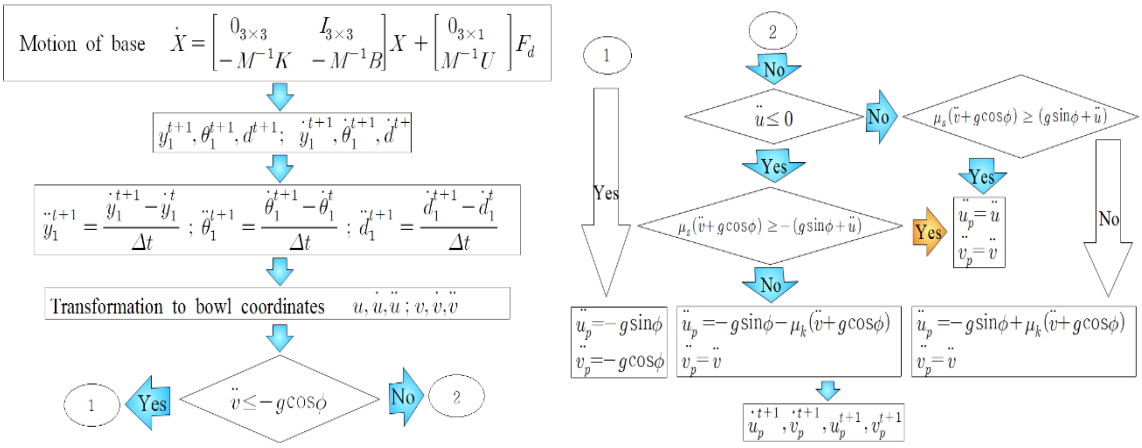

(a) Base and Bowl Motion (b) Part Motion

Figure 5: Flow Chart to Obtain the Part Acceleration and Velocity from the Bowl Motion.

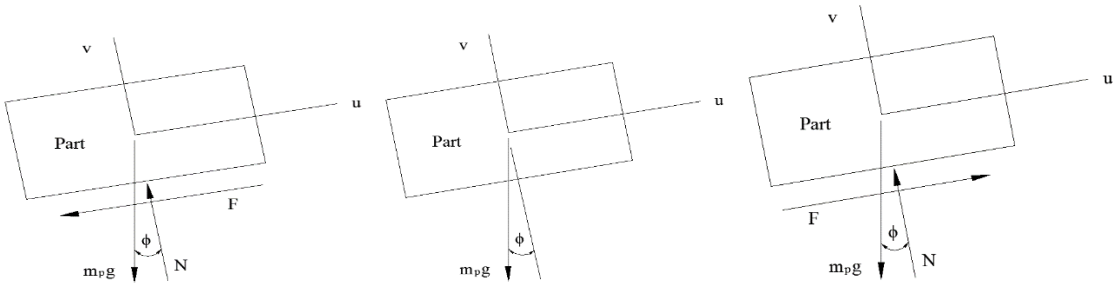

(a) Forward Slip (b) Backward Slip (c) Jump

Figure 6: Relative Motion of the Part on the Track of the Bowl.

3. ANALYSIS OF THE EXCITATION FORCE AND MOTION OF THE BOWL FEEDER

In the analysis of the excitation force, as the design parameters of electromagnet, the number of coil turns was 3,000, the length of core was 171 mm, the relative permeability of the core was 3,000, the permeability of air was $4\pi \times 10^{-10}\ H/mm$, the sectional area of the core was 199.5 mm^2, and the resistance of the coil was 167.6 Ω. With the proposed equation of excitation model, the excitation force and coil current were analyzed with variations of voltage of 80~220 V in amplitude, frequency of 40~220 Hz, and air gap of 0.3~1.0 mm.

The base of the proposed bowl feeder was made of structural steel (SS440), and the bowl was made of aluminum (Al2025). The main design parameters of the bowl feeder were as follows: mass of base was 4.604 kg, leaf spring angle relative to horizon was 75º, mass of bowl was 2.082 kg, angle of inclination was 2º.

The motion analysis of the bowl feeder was carried out for 0.5 s just after the excitation start, using a numerical method on the equation through the procedure presented in figure 5 with total solution steps of 30,720. In the analysis, the

part was assumed to move through the center of the track positioned at a radius of 70 mm from the center of the bowl. The static and dynamic friction coefficients were assumed to be 0.95 and 0.9, respectively. In the motion analysis, the air gap in the electromagnet was set to be constant at 0.5 mm, the voltage magnitude was set to change from 120 V to 220 V, and the frequency of excitation was set to change from 40 Hz to 80 Hz.

4. RESULTS AND DISCUSSIONS

The effects of voltage magnitude, frequency, and air gap on the current and attractive force of the electromagnet are analyzed respectively using the proposed model to reveal the results shown in figure 7. Figure 7(a) shows that as the voltage magnitude increases to 220 V, the current and the attractive force are also increased linearly to about 310 mA and 400 N, respectively. Figure 7(b) shows that when the frequency increases from 45 Hz to 210 Hz, the current and the attractive force decrease parabolically from 350 mA to 70 mA and 500 N to 20 N, respectively. Figure 7(c) shows that as the air gap increases from 0.3 mm to 1.0 mm, the current is increased linearly from 180 mA to 520 mA, whereas the attractive force is decreased slowly from 350 N to 290 N. According to the results, to obtain the higher attractive force, the voltage magnitude should be increased, but the frequency should be reduced. The change of air gap did not have much influence on the attractive force.

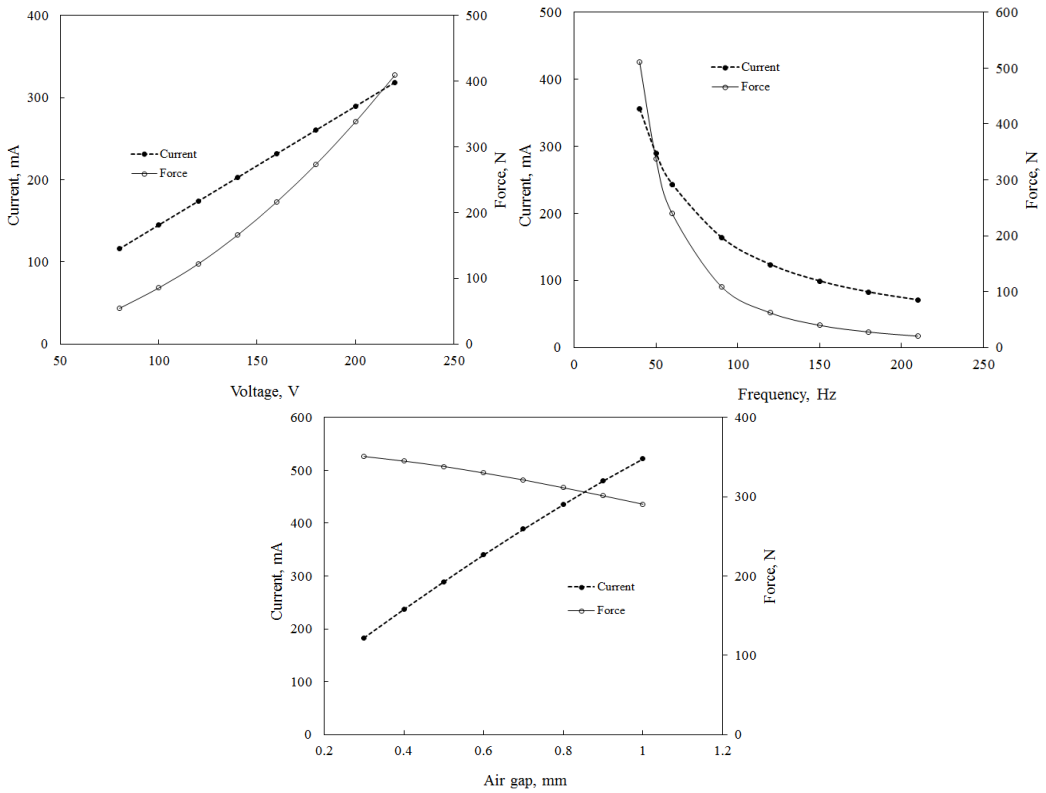

(a) Effect of Voltage (b) Effect of Frequency (c) Effect of Air Gap

Figure 7: Effect of the Electromagnet Variables on the Coil Current and Attractive Force.

Figure 8(a) shows that when the voltage magnitude increases from 120 V to 220 V with keeping the frequency at 50 Hz, the vertical displacements of the bowl are expected to change. At 0.03 s after the start of excitation, the displacement begins to settle down to a constant magnitude, which is related to the voltage magnitude applied. When the voltage reaches 220 V, the displacement has a magnitude in the range of -0.045 ~ 0.023 mm. The bowl presents a downward displacement with the attractive force of the electromagnet, while the opposite displacement occurs by both the

spring force of the leaf springs, and the inertial force when the attractive force diminishes periodically. When the voltage magnitude increases from 120 V to 200 V, the displacements of the part on the track increase with elapsed time, and the incremental slopes of the displacements change in proportion to the voltage, as shown in figure 8(b). With the result of displacement, the feed rate of the part can be obtained. When the magnitudes are 120 V and 200 V, the feed rates are about 7 mm/s and 19 mm/s, respectively. Meanwhile, as the voltage magnitude increases, a saw tooth shape is presented at the result of the part displacement, that is, a partial reduction of the displacement occurs periodically. This is because of the periodical backward motion during the mainly forward movement of the part.

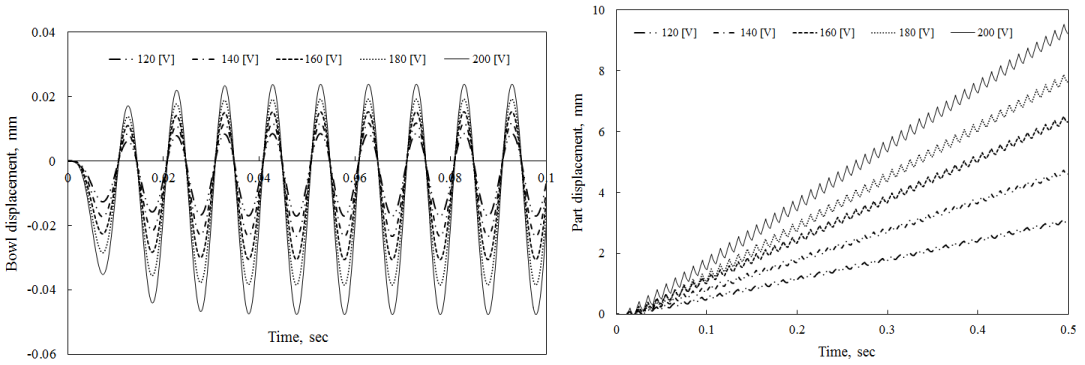

(a) Bowl Displacement (b) Part Displacement

Figure 8: Displacement of the Bowl and Part During the Vibratory Feeding with Various Excitation Voltages.

When the applied voltage is of 160 V and 50 Hz, the velocity and travel patterns (arbitrary scale: 20) in the u direction of the bowl and part are predicted as shown in figure 9. Figure 9(a) shows that when the speed of the bowl is greater than that of the part, the part slips backward, whereas when the speed of the part is greater than that of the bowl, the part slips forward. In the figure, the forward slip portion is somewhat greater than the backward slip portion in each cycle, feeding the part forward continuously. At 0.03 s after the excitation, the motions seem to be stable, and repeat with the same oscillatory patterns. In particular, the jump travel of the part occurs periodically during forward slip motion. Before and after the slip travel motion, short terms of static travel are presented periodically, showing no slip between the bowl and part. Figure 9(b) shows the predicted acceleration and travel pattern (arbitrary scale: 5,000) of the bowl and the part at the same time. The acceleration of bowl in the u direction is 3 times greater than that in the v direction, and 2 times greater than that of the part in the u direction. The part happens to slip backward when the acceleration of the bowl in the u direction is positive. This is because of the inertia of the part traveling on the track of the bowl. The part also accelerates forward periodically, even though backward motion just relative to the bowl occurs. The speed of the part in the period increases as shown in figure 9(a). Meanwhile, the part slips forward, and its acceleration in the u direction decreases to nearly 0, due to the inertia when the acceleration of the bowl in the u direction is negative. This can be matched to the constant speed of the part in the corresponding period, as shown in figure 9(a). When the acceleration of the bowl in the u direction is negative, and that of the bowl in the v direction becomes less than $g\cos\emptyset$ at the same time, the part moves forward with jump motion, and has the acceleration of $g\sin\emptyset$. As the applied voltage increased from 120 V to 220 V, the positive acceleration also increased, whereas the negative acceleration largely decreased, and finally reached as a small magnitude as $g\sin\emptyset$ in a period where a jump travel of the part happened to occur.

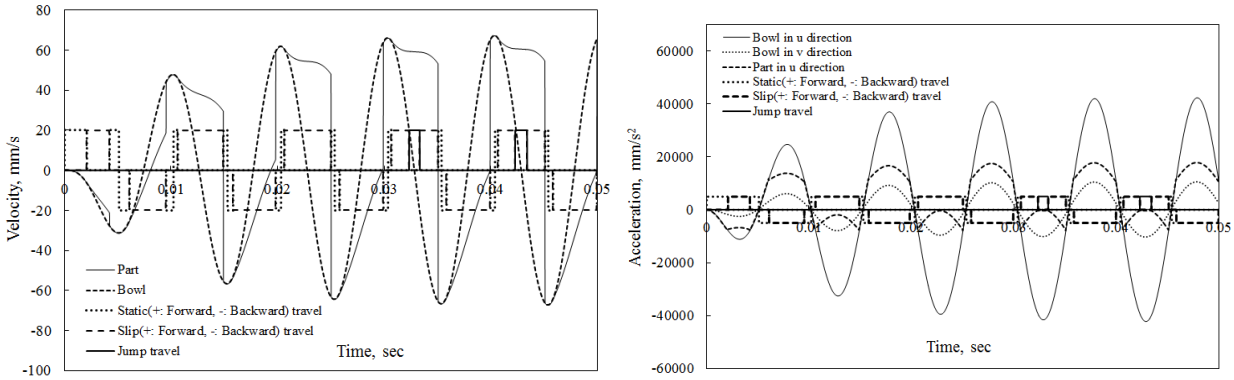

(a) Velocity in the u Direction (b) Acceleration

Figure 9: Motion of the Bowl and Part in Vibratory Feeding.

When the frequency is changed from 40 Hz to 80 Hz, with a constant voltage magnitude of 200 V, the changes of the vertical displacement of the bowl are predicted as shown in figure 10(a). The bowl is loaded to have a negative displacement by the attractive force, and moves to have a positive displacement by the resilience of the leaf springs when the force diminishes. At 40 Hz, the displacement has the range from -0.062 mm to 0.025 mm. The magnitude of the displacement decreases as the frequency increases, and the displacement has the range from nearly zero to 0.008 mm at a frequency of 80 Hz. Figure 10(b) shows the predicted displacements of the part with the change of the frequency. The displacement increases linearly with the elapsed time, and the feed rate can be calculated as 20 mm/s at a frequency of 40 Hz. As the frequency decreases to 50 Hz, the feed rate is increased. However, when the frequency changes from 50 Hz to 40 Hz, the feed rate is not much increased.

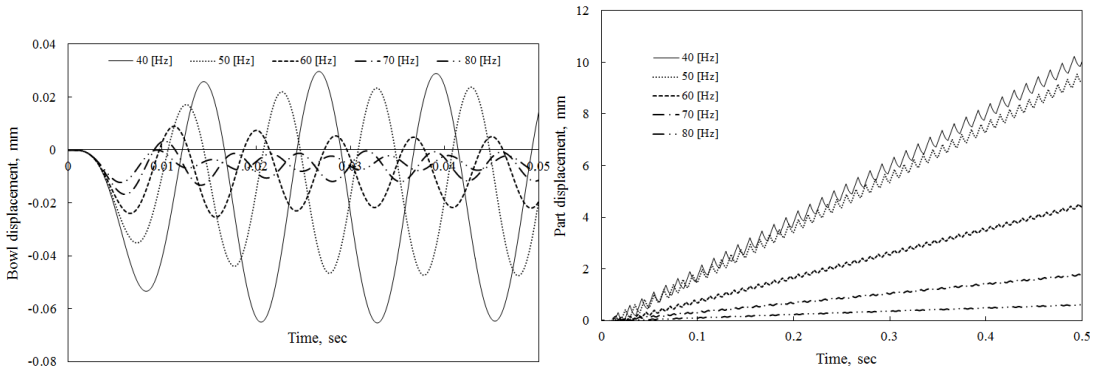

(a) Bowl Displacement (b) Part Displacement

Figure 11: Displacement of the Bowl and Part During the Vibratory Feeding with Various Excitation Frequencies.

The acceleration and travel pattern of the part that were also predicted when the frequency was changed from 40 Hz to 60 Hz. When the frequency was 40 Hz or 50 Hz, the part traveled on the track mainly with the jump motion, and partially with the slip motion; whereas when the frequency was 60 Hz, the part traveled only with the slip motion.

5. CONCLUSIONS

In the design of a vibratory bowl feeder for handling thin plastic discs of 50 μm thickness, the excitation force of the electromagnetic was modelled, and the dynamics of the bowl and part were analyzed with the variations of voltage of 80~220 V, frequency of 40~220 Hz, and air gap of 0.3~1.0 mm. With the force model and the dynamic analysis, the following conclusions were made:

- As the frequency of the supply voltage increased, the excitation force and current of the electromagnet decreased parabolically; whereas as the magnitude of the voltage increased, they increased linearly.
- As the gap between the cores of the magnet increased, the current of the electromagnet increased linearly and the excitation force decreased a little, even though the gap size did not affect the magnitude of the bowl vibration.
- As the frequency of the supply voltage decreased, the magnitude of bowl vibration and the part feed rate increased. Meanwhile, the feed rate saturated around the maximum value.
- When the magnitude of the supply voltage was low, the part moved with slip motion; whereas, when the magnitude were large enough, the part moved with jump motion.
- When the frequency of the excitation voltage was high, the part moved mainly with slip motion; however, as the frequency decreased, the part moved mainly with jump motion.

REFERENCES

1. *Deshmukh, T. (2017). Performance Analysis of a Vibratory Bowl Feeder, International Journal of Current Engineering and Technology, 7(5), 1741-1744*
2. *Boothroyd, G., Poli, C., & Murch, L. E. (1982). Automatic Assembly, Ch. 3 Vibratory Bowl Feeders, Marcel Dekker, Inc., New York and Basel*
3. *Han, I.-H., Lee, Y.-J., & Yoon, K.-Y. (1996). Numerical Study on Chaotic Dynamics of Repeated Impacts with Friction - Vibratory Bowl Feeders, Journal of the Korean Society of Precision Engineering, 13(1), 143-152*
4. *Kim, S.-C., Kim, H.-N., & Kwon, D.-H. (1996). A Study on the Vibration Characteristics for Parts Feeder, Journal of the Korean Society of Machine Tool Engineers, 5(1), 17-26*
5. *Hsieh, W. H., Lin, G.-H., & Tsai, C.-H. (2013). Kinematic Analysis of a Novel Vibratory Bowl Feeder, Vibroengineering Procedia, Vibroengineering, 2(11), 92-97*
6. *Ashrafizadeh, H., & Ziaei-Rad, S. (2013). A Numerical 2D Simulation of Part Motion in Vibratory Bowl Feeders by Discrete Element Method, Journal of Sound and Vibration, 332, 3303-3314*
7. *Maul, G. P., & Tomas, M. B. (1997). A Systems Model and Simulation of the Vibratory Bowl Feeder, Journal of Manufacturing Systems, 16(5), 309-314*
8. *Sturm, M., & Pesik, L. (2017). Determination of a Vibrating Bowl Feeder Dynamic Model and Mechanical Parameters, Acta Mechanica et Automatica, 11(3), 243-246*
9. *Lee, S.-B., & Noh, C.-J. (1979). A Study on the Comparison of Attracting Force of AC Solenoid Coil with that of DC Solenoid Coil, Journal of Korea Maritime and Ocean University, 14(3), 7-13*
10. *Park, S.-B. (1994). Circuit Theory, Moonundang, Ch. 2.*